The Korean Journal of Ceramics, **5** [2] 189 - 194 (1999)

Crystalline Phases and Dielectric Properties of Crystallized Glasses in the System (Ca, Sr, Ba)O-Al_2O_3-B_2O_3-SiO_2-TiO_2

Koichiro Tuzuku*,, Hiroshi Kishi*, Seiichi Taruta** and Nobuo Takusagawa****

**Taiyo Yuden Co., Ltd., Nakamuroda 5607-2, Gunma 370-3347, Japan*
***Shinshu Univ., Wakasato 500, Nagano-shi, Nagano 380-0922, Japan*
(Received September 23, 1998)

Crystallization of glasses in the system (Ca, Sr, Ba)O-Al_2O_3-B_2O_3-SiO_2-TiO_2 and dielectric properties of crystallized glasses were investigated. As increasing B_2O_3 content and decreasing SiO_2 content in the glass, the major crystalline phase changed from (Sr, Ba)$_2TiSi_2O_8$ to (Ca, Sr, Ba)TiO_3, the dielectric constant of crystallized glasses increased and the Temperature Coefficient of Capacitance (TCC) changed to negative. The dielectric constant and TCC was estimated for (Sr, Ba)$_2TiSi_2O_8$ phase as 18 and -440 ppm/°C, respectively and for (Ca, Sr, Ba)TiO_3 phase as 307 and -1900 ppm/°C, respectively. The dielectric properties of (Ca, Sr, Ba)TiO_3 phase (in this study) were similar to those of (Ca, Ba)TiO_3 solid-solution[12], but (Sr, Ba)$_2TiSi_2O_8$ phase (in this study) and $Sr_2TiSi_2O_8$[4] showed the different properties.

Key words : Glass-Ceramics, Dielectrics, Temperature Coefficient of Capacitance

I. Introduction

The glass ceramics method, by which glass is converted to micro-crystalline materials by heat treatment, has the advantage of producing dense polycrystals at a comparatively lower temperature. Therefore, the glass-ceramic method have been applied to manufacturing such as low temperature sintered multilayer substrates.[1-3] And it has already reported that electrical properties such as piezoelectric and/or pyroelectric properties can be designed by controlling the precipitation of crystalline phases.[4] If dielectric properties, such as dielectric constant and/or temperature coefficient of capacitance, could be designed by the same technique, the fabrication of dielectrics with co-firable internal electrode is feasible even at lower temperature. Already, there are several reports on evaluation of glass-ceramics and resultant dielectric properties.[5,6] To employ these materials for dielectrics, it is required that Temperature Coefficient of Capacitance (TCC) can be controlled between+100 ppm/°C and -300 ppm/°C. Common glasses, such as alkaline borosilicate glass and soda-lime glass, and their crystallized products, show positive value of TCC[7] at room temperature, for that reason it is only a limited case to use thesematerials as dielectrics.

There are two methods for controlling TCC of these materials, the first is a composite method; glasses having positive TCC value and compounds having negative TCC value (ex. TiO_2, $CaTiO_3$, $SrTiO_3$) are mixed, and the second is a crystallization method;[8] crystals having negative TCC value precipitate in glasses. In general, the crystallization method has the advantage to produce dielectrics having homogeneous texture more than the composite method.

In this study, to promote homogenous crystallization of glass, TiO_2 as nucleation agent was added to (Ca, Sr, Ba) O-Al_2O_3-SiO_2 glasses. Furthermore, in order to decrease viscosity and to promote crystallization of glasses SiO_2 component in the glasses was partially substituted by B_2O_3 at different ratios. And, relationships between precipitated phases and resultant dielectric properties of crystallized glasses were studied.

II. Experimental Procedure

1. Preparation of samples

Chemical composition of the samples were shown in Table 1. Sample B0 did not contain B_2O_3 and samples B10-B40 contained B_2O_3, in which B_2O_3 substituted for SiO_2 in different mole ratio of B_2O_3/SiO_2. Raw materials of $CaCO_3$, $SrCO_3$, $BaCO_3$, Al_2O_3, SiO_2, B_2O_3 and TiO_2, were mixed in the ratios corresponding to the chemical composition of samples B0-B40. These mixtures were melted in alumina crucibles at 1400°C or 1500°C for 0.5 hr as shown in Table 1 and quenched on a steel plate. Obtained glassy samples were powdered with an impact mill under 44 μm in size. Mean diameter of powdered glass samples were shown in Table 2. These powders were pressed into disks, 10 mm in diameter and 0.8 mm in thickness, and sintered at 850°C, 900°C or 950°C for 2 hr in air after being heated up from room temperature to each temperature at the heating rate of 5°C/min.

2. Characterization of samples

Glass transition temperatures and crystallization tem-

Table 1. Chemical Compositions of Sample Glasses

Sample	Elements (mol%)							Melting Temperature (°C)
	CaO	SrO	BaO	Al_2O_3	SiO_2	$BO_{1.5}$	TiO_2	
BO	6.5	17.9	10.0	8.4	46.4	0.0	10.8	1500
B10	6.5	17.9	10.0	8.4	41.8	4.6	10.8	1500
B20	6.5	17.9	10.0	8.4	37.1	9.3	10.8	1500
B30	6.5	17.9	10.0	8.4	32.5	13.9	10.8	1500
B40	6.5	17.9	10.0	8.4	27.8	18.6	10.8	1400

Table 2. Mean Diamter of Glass Powders

Sample	Mean Diameter (μm)
B0	6 7
B10	5.8
B20	6 1
B30	6.0
B40	6.4

peratures of powdered glass samples were examined with Differential Scanning Calorimeter (Seiko Ins. Inc. DSC) at the heating rate of 20°C/min. Crystallized phases in sintered samples were identified with X-ray Diffractmeter (Rigaku XRD) and these microstructures were observed with Scanning Electron Microscope (Hitachi FE-SEM; S-4000). Dielectric properties of sintered samples were measured using Ag electrode and LCR meter (HP 4284A) at temperatures ranging from -55°C to +125°C.

III. Results and Discussion

1. Differential thermal analysis

The temperature, at which endo-therm begins on DSC curve, corresponds to the glass transition temperature (Tg) and the temperature of exo-thermal peak (Tp) is crystallization temperature. Observed temperatures of Tg and Tp were indicated on each DSC curve (Fig. 1). As increasing B_2O_3 content and SiO_2 content decreased in glass, Tg decreased from 753°C (B0) to 654°C (B40) and also Tp decreased from 980°C (B0) to 838°C (B40). In addition, exo-thermal peak of samples B30-40 decreased in height and became broad profile.

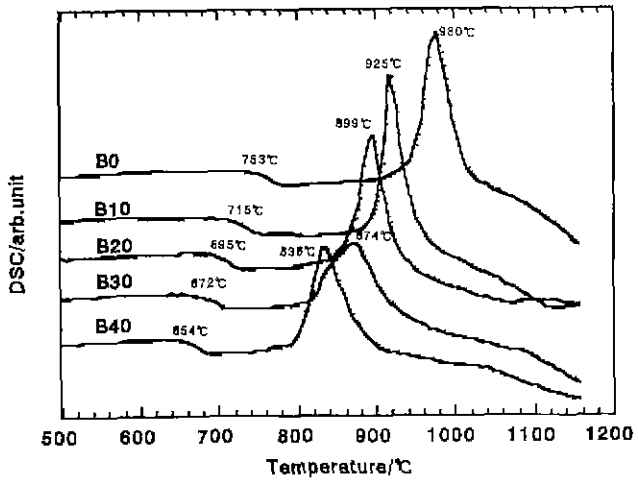

Fig. 1. DSC curves of powdered samples B0-B40 at the heating rate of 20°C/min.

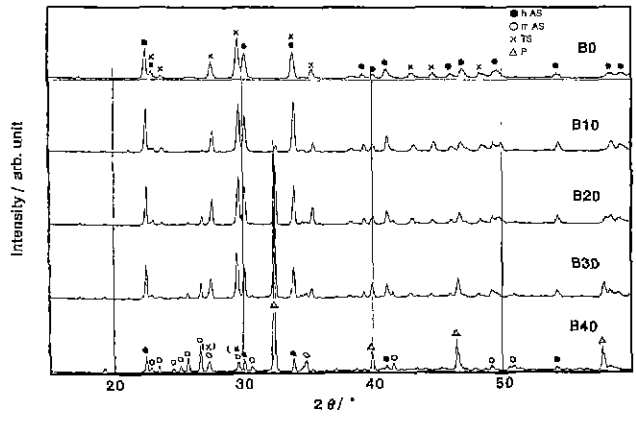

Fig. 2. XRD patterns of samples B0-B40 sintered at 900°C for 2 hr. h-AS: hexagonal (Ca, Sr, Ba)$Al_2Si_2O_8$, m-AS: monoclinic (Ca, Sr, Ba)$Al_2Si_2O_8$, TS: (Sr, Ba)$_2TiSi_2O_8$, P: ($Ca_{0.4}$, $Sr_{0.2}$, $Ba_{0.4}$)TiO_3.

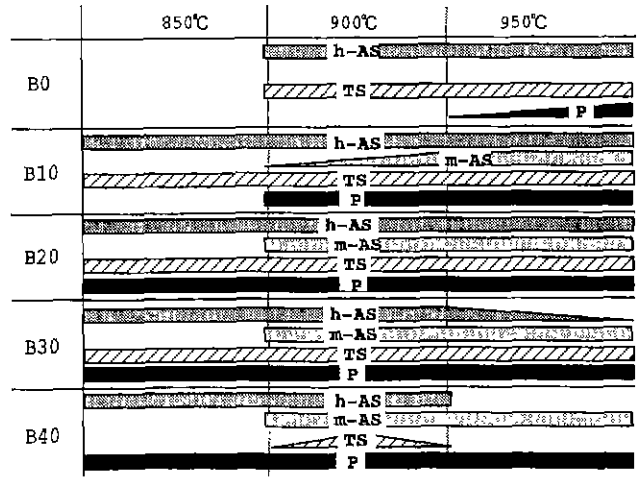

Fig. 3. Crystallized phases in samples B0-B40 at 850°C~950°C. h-AS: hexagonal (Ca, Sr, Ba)$Al_2Si_2O_8$ phase, m-AS: monoclinic (Ca, Sr, Ba)$Al_2Si_2O_8$ phase, TS: (Sr, Ba)$_2TiSi_2O_8$ phase, P: ($Ca_{0.4}$, $Sr_{0.2}$, $Ba_{0.4}$)TiO_3 phase.

2. *Crystallized phases*

Crystallized phases were identified by XRD method for the samples sintered at 850°C, 900°C or 950°C. XRD profiles of the samples sintered at 900°C were shown in Fig. 2. (Sr, Ba)$_2$TiSi$_2$O$_8$ [TS], perovskite (Ca, Sr, Ba)TiO$_3$ [P], hexagonal and monoclinic (Ca, Sr, Ba). Al$_2$Si$_2$O$_8$ [h-AS, m-AS] were precipitated in these samples. Fig. 3 shows crystallized phases in the samples sintered at different temperatures.

Crystallized phases varied with sintering temperature and content of B_2O_3. In the sample B0, which did not contain B_2O_3, crystallization did not occur at 850°C. TS and h-AS phases precipitated in the sample B0 at 900~950°C. In the samples containing B_2O_3 crystallization occurred even at 850°C. In the sample B10, h-AS and TS precipitated at 850~950°C, while m-AS and P precipitated at 900~950°C.

As increasing the B_2O_3 content P increased in sintered samples. In the samples B20-30, h-AS, TS and P precipitated at 850~950°C, m-AS appeared and h-AS decreased at 900°C and 950°C. In the sample B40, which contained the largest amount of B_2O_3 among the used samples, P precipitated at 850~950°C, h-AS and m-AS precipitated at 850~900°C and at 900~950°C, respectively.

3. *Microstructure of sintered samples*

SEM photographs of fractured surface of samples sint-

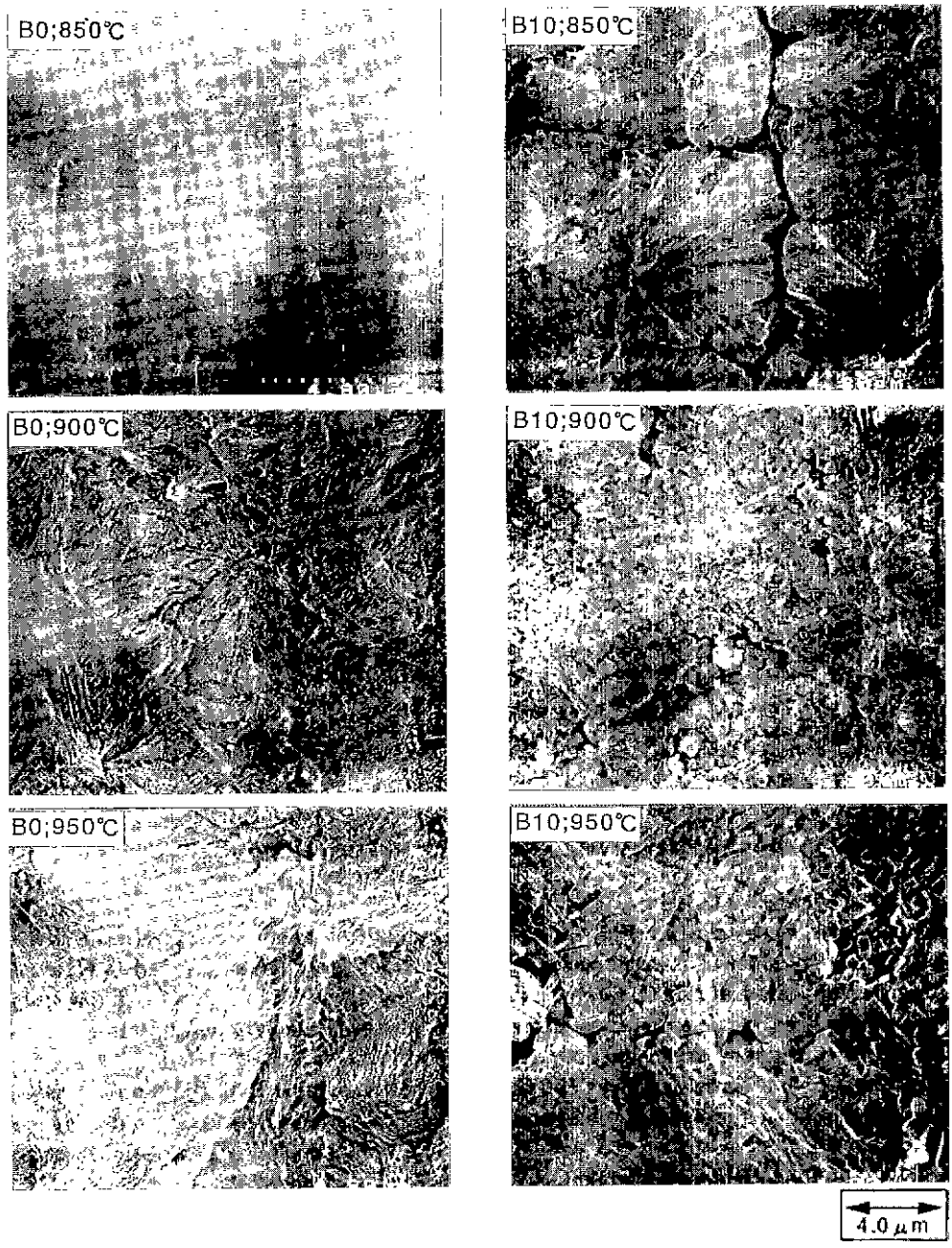

Fig. 4A. SEM photographs of the fractured and chemical etched surface of samples B0 and B10, sintered at 850~950°C for 2 hr.

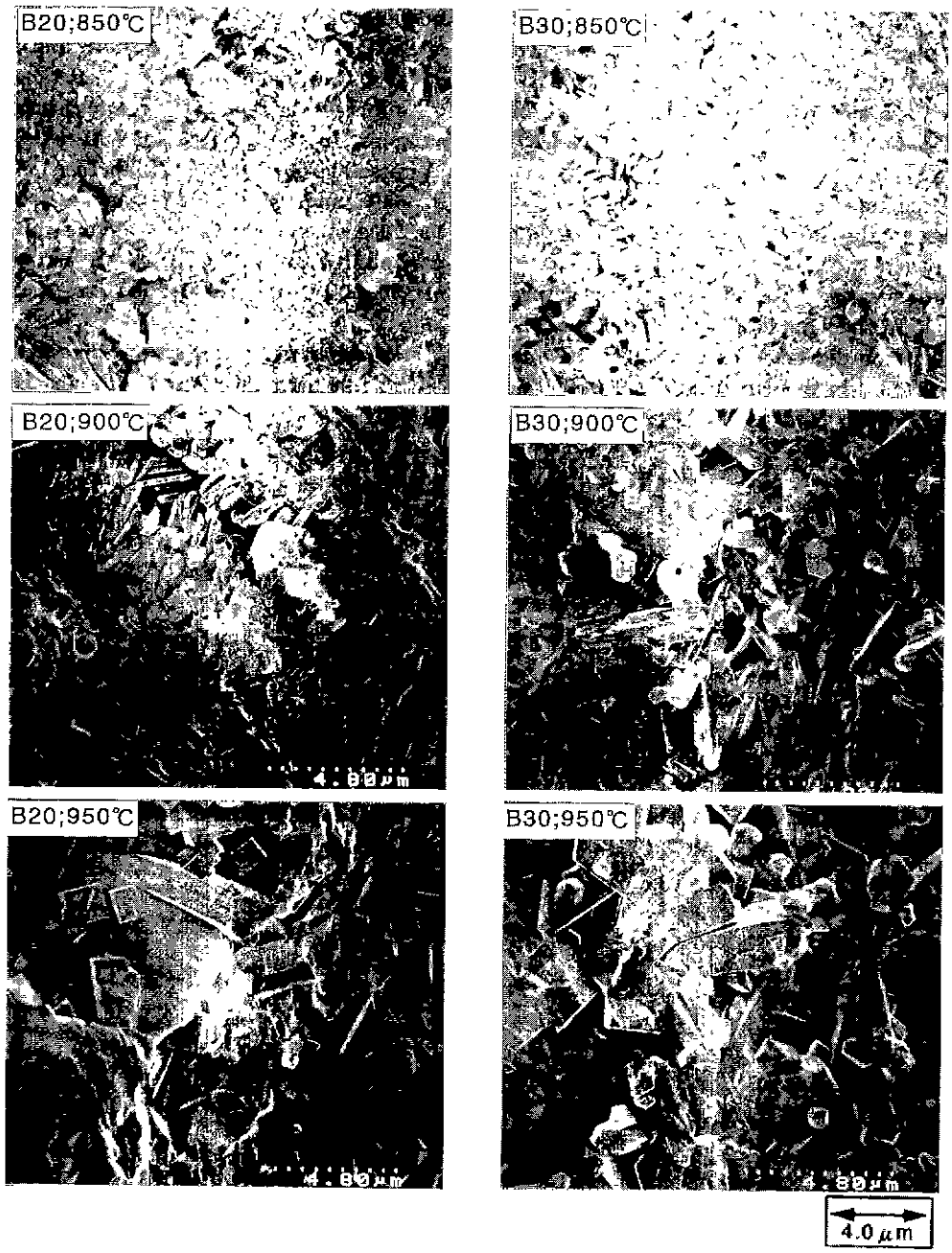

Fig. 4B. SEM photographs of the fractured and chemical etched surface of samples B20 and B30, sintered at 850~950°C for 2 hr.

ered at different temperatures were shown in Fig. 4.

In the sample B0, a small number of microparticles of about 0.2 μm in diameter appeared at 850°C, however it was difficult to determine these particles as crystalline phases, and dendritic arrangement consisted of microparticles formed at 900°C, which grew larger at 950°C. Those particles were expected being crystalline phases of TS and h-AS.

In the sample B10, the dendritic arrangement appeared at 850°C, each particle grew larger at higher temperatures and the dendritic arrangement disappeared.

In the sample B20, a larger number of particles of 0.5~1 μm in diameter precipitated at 850~900°C and these particles grew larger plate or rod-like particles of 1~2 μm in length at 950°C. Also a small number of polygonal particles of about 2 μm in diameter precipitated at 850~950°C.

In the sample B30, the plate or rod-like particles grew 1~2 μm in length at 850°C and increased in the width at 900°C and 950°C. Also a number of polygonal particles coexisted at 850~950°C.

In the sample B40, microparticles of 0.3~0.5 μm in diameter and plate or rod-like particles of 1~2 μm in length having width of about 0.3 μm appeared at 850°C.

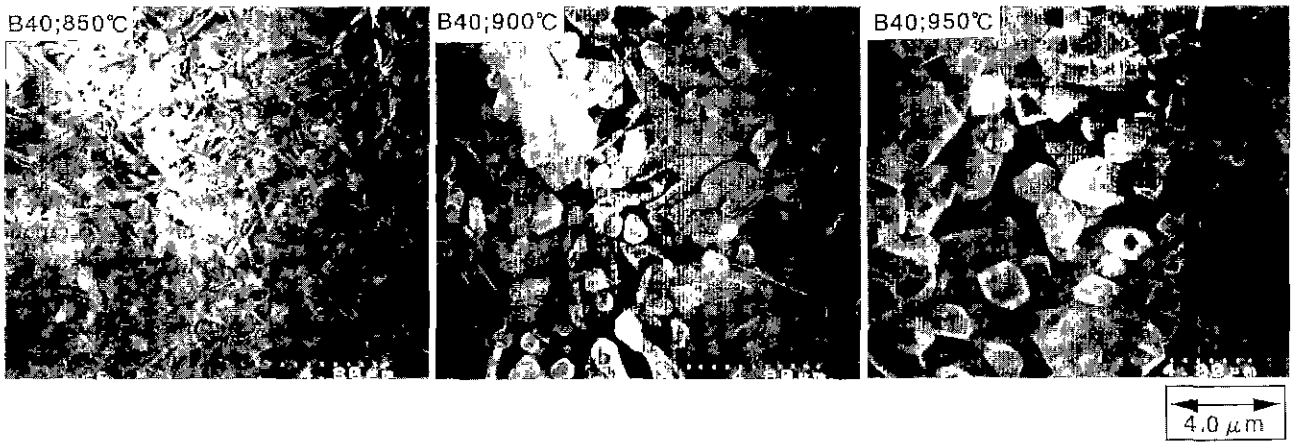

Fig. 4C. SEM photographs of the fractured and chemical etched surface of sample B40, sintered at 850~950°C for 2 hr.

These microparticles increased in diameter up to 1 μm, plate or rod-like particles grew 2 μm in length and a number of larger particles of several micrometer in size appeared at 900°C. Microparticles of about 0.7 μm in diameter, polygonal particles of 1~2 μm in diameter and larger plate or rod-like particles of 5~10 μm in length appeared at 950°C. The amount of residual glassy phase was a few in the samples B0-30, however, a considerable amount of glassy phase appeared at 950°C in the sample B40 in which only two phases of P and m-AS precipitated.

The results of XRD analysis and SEM observation show that microparticle is TS phase, smaller and larger plate or rod-like particles are h-AS and m-AS phase respectively, and polygonal particle is P phase.

4. The dielectric properties of the crystallized samples

The temperature dependencies of capacitance (TCC) of samples B0-B40 sintered at 900°C for 2 hr were shown in Fig. 5. The dielectric constant at 20°C and the TCC of the samples B0-B40 sintered at 850~950°C for 2 hr were summarized in Table 4. As increasing B_2O_3 content, TCC changed toward negative and dielectric constant increased monotonously. Comparing the precipitated phases in samples B0-B40, it was considered that these changes of dielectric properties were caused by the decrease of TS phase and the increase of P phase.

The dielectric properties of TS phase and P phase were

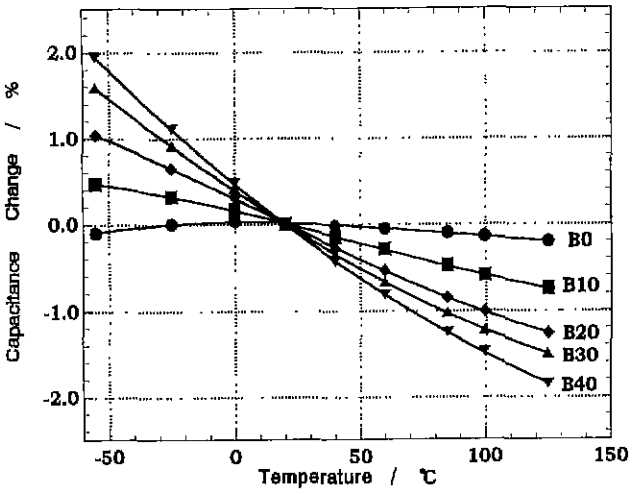

Fig. 5. *Temperature dependencies of the change in capacitance* for the samples B0-B40 sintered at 900°C for 2 hr.

estimated using the mixed mol ratio of raw materials (Table 1), the precipitated phases (Fig. 3), the morphology of crystals (Fig. 4) and the dielectric properties (Table 3). For a complex composed of some components, the dielectric constant can be calculated by "logarithmic mixture rule",[10] if interactions among components could be ignored. And also, it is known empirically that the temperature dependence of dielectric constant conforms to "mole-ratio mixture rule".[11] Calculation was carried out under the

Table 3. Temperature Coefficient of Capacitance (TCC) and Dielectric Constant (ε_r) of Sampes B0-B40

Sample	850°C		900°C		950°C	
	TCC (ppm/°C)	ε_r	TCC (ppm/°C)	ε_r	TCC (ppm/°C)	ε_r
B0	120	10.8	-19	11.5	-70	11.3
B10	9.5	11.8	-71	11.9	-104	11.9
B20	-112	13.1	-120	12.9	-103	13.0
B30	-203	13.9	-143	13.9	-124	13.6
B40	-270	15.1	-176	14.8	-190	14.2

Table 4. Estimated Dielectric Constant (ε_r) and Temperature Coefficient of Capacitance (TCC) for TS Phase and P Phase with the Data for Comparing

Phases	ε_r at 20°C	TCC (ppm/°C)
h-AS/m-AS phase	8.9	+142
glass phase (=B0; 850°C)	10.8	+120
TS phase	18	-440
P phase	307	-1900
$Sr_2TiSi_2O_8$[4]	11.5	no defined
$CaTiO_3$[13]	170	-1600
$SrTiO_3$[13]	250	-3000
$(Ca_{0.6}Ba_{0.4})TiO_3$[13]	~220	negative
$BaTiO_3$[13]	1500	ferroelectrics

conditions shown as follows.

1) All of TiO_2 component in the glasses crystallized as TS phase and/or P phase.

2) All of Al_2O_3 component in the glasses crystallized as h-AS phase and/or m-AS phase.

3) The dielectric properties of h-AS phase were the same as those of m-AS phase (dielectric constant=8.9, TCC=+141 ppm/°C).[12]

4) Percent crystallinity of the samples B0 sintered at 950°C, B40 sintered at 850°C and 950°C were 90% which were estimated from Fig. 4. The sample B0 sintered at 850°C was not crystallized.

5) The dielectric properties of glass phase was the same as of the sample B0 sintered at 850°C (dielectric constant=10.8, TCC=+120 ppm/°C).

The dielectric properties of TS-phase was calculated using those values of the sample B0 sintered at 850°C or 950°C, in which only a glassy phase or h-AS and TS phases were contained, respectively. The dielectric properties of P phase was calculated using those values of the sample B40 sintered at 850°C or 950°C, in which h-AS and perovskite phases or m-AS and perovskite phases were contained, respectively. The dielectric constants of TS phase, P phase, $Sr_2TiSi_2O_8$[4], $CaTiO_3$,[13] $SrTiO_3$,[13] $BaTiO_3$[13] were summarized in Table 4.

The calculated dielectric constant of TS phase was larger than that of $Sr_2TiSi_2O_8$ phase shown in reference no. 4. The calculated dielectric constant of P phase was lrger than that of $SrTiO_3$, each phases have cubic structure, and TCC of P phase was smaller than that of $SrTiO_3$. Difference in dielectric constant between TS phase and $Sr_2TiSi_2O_8$ phase was not enough analyzed, yet. But, it was considered that the dielectric properties of the precipitated P phase were comparable to those of (Sr, Ba)TiO_3 shown in reference no. 13.

IV. Conclusion

The compacted powders of (Ca, Sr, Ba)O-Al_2O_3-B_2O_3-SiO_2-TiO_2 glasses, in which different amount of B_2O_3 were added substituting for part of SiO_2 component, were crystallized and those dielectric properties were investigated. The results are as follows:

1) As increasing B_2O_3 content, crystallization temperature decreased and dense crystallized products were obtained at lower temperature.

2) As increasing B_2O_3 content, TS phase decreased and P phase increased, also h-AS phase decreased and m-AS phase increased at higher temperatures.

3) The dielectric constant and TCC was estimated for TS phase as 18 and -440 ppm/°C, respectively and for P phase as 307 and -1900 ppm/°C, respectively.

4) The dielectric properties of sample B40 sintered at 850~950°C for 2 hr conformed to RH class (range in TCC is -220 ppm/°C±60 ppm) in EIAJ (Electrical Industry Association Japan) Standard.

References

1. S. Nishigaki and K. Noda, FC Report **6**(11), (1988).
2. Ceramic-Kiban to sono ouyou, New Kerass, No. 4 Gakk-en-Sha. (1988).
3. A. Imoto and K. Furuhashi, Cercuit Technology **9**(7), (1984).
4. Glasses and Glass-Ceramics, M. H. Lewis (Ed.), Chapman and Hall, (1989)
5. T. Kokubo, H. Nagao and M. Tashiro, Yogyo-Kyokai-Shi, **77**(9), 293 (1969).
6. K. Hayashi, Y. Nishioka and Y. Okamoto, *J. Ceram. Soc. Jpn.*, **98**(8), 801 (1990).
7. A. G. Cockbain and P. J. Harrop, *Brit. J. Appl. Phys.*, **2**(1), 79 (1968).
8. K. Tuzuku, and N. Takusagawa, Ceramics Research Conference of Kanto Branch 11th (1995).
9. N. P. Bansal and C. H. Drummoond, *J. Am. Ceram. Soc.* **76**(5), 1324 (1993).
10. W. D. Kingery, H. K. Bowen, D. R. Uhlmann, Introduction to Ceramics 2nd Ed., pp.947, John Willy & Sons, Inc., New York (1975).
11. K. Tuzuku, Private data.
12. K. Tuzuku, Proc., Fall Meeting of Ceram. Soc. Jpn. (1994).
13. LANDOLT-BORNSTEIN vol. 3, Springer-Verlag (1969).